Mechanical Spallation of Charring Ablators in Hyperthermal Environments

RICHARD D. MATHIEU*
General Electric Company, Philadelphia, Pa.

Analytical results are presented for the transient ablation performance of a high-performance castable ablation resin for which spallation is responsible for the char removal. The mechanism for the spallation process is assumed to depend upon the internal stress due to the gas pressure drop through the char and a critical char thickness that is related to the surface shear stress. The environmental conditions considered are representative of a ballistic re-entry trajectory. Detailed calculations of the temperature, gas pressure, material density, porosity, and stress distribution through the material are presented. The effect of the char porosity on the internal stress is shown. In addition, results that demonstrate the effects of increased heating on the char removal and over-all ablation performance are presented.

Nomenclature

A = frequency factor
B_1, B_2 = constants in Eq. (7)
C_p = specific heat
E = activation energy
f = porosity
H_k = heat of degradation
k = thermal conductivity
K = permeability
L = initial thickness
$\dot{m}$ = mass flux
$\bar{M}$ = molecular weight
n = order of degradation reaction
p = pressure
q = heat flux
R = universal gas constant
t = time
T = temperature
$\dot{W}_p$ = rate of plastic degradation
x = distance normal to surface
δ = char thickness
ρ = density
Γ = gasification ratio
σ = normal stress
τ = shear stress

Subscripts

VP = virgin plastic
c = mature char
w = surface
g = gas
s = solid material

Introduction

UPON exposure to ballistic re-entry and rocket nozzle environments, heat-protection materials are subjected to severe thermal and mechanical conditions. Various heat protection systems (heat sink, transpiration or mass transfer cooling, ablation) have been proposed and investigated quite extensively, especially from the experimental viewpoint. Ablation heat-protection systems, which are characterized by the sacrificial removal of the surface material for the protection of the underlying structure, have been the most promising to date and have been applied successfully to the re-entry and rocket nozzle problems. Reviews of recent experimental and theoretical investigations concerning several classes of ablation materials have been given by Steg and Lew[1] and by Hurwicz.[2]

The charring ablators constitute one of the most important classes of materials, because these materials provide a relatively efficient heat-protection system through a variety of heat-absorbing mechanisms, which occur during the over-all ablation process. Initially, the material absorbs the heat it is exposed to, and the temperature rises. As the temperature continues to increase, the material undergoes thermal degradation. Gases are formed and a porous carbonaceous char remains. As the process continues, the degradation zone moves into the material. The degradation gases flow through the porous char to the surface and tend to cool the surface. At the same time, the gases interact with the external flow, reducing the heat flux and shear stresses at the surface because of the mass addition effects. The char layer also has an insulating effect, and as it becomes thicker, the heat flux to the undegraded material is reduced. Thus, the flow of gases decreases as the degradation process slows down allowing the surface temperature to rise again. At the higher temperature, heat is reradiated from the surface. The char is finally removed by one or several erosion mechanisms such as sublimation, oxidation, or intermittent spallation due to the mechanical and thermal stresses.[3] Thus, the over-all ablation process of these materials is quite complex, but highly desirable because of the relatively high ablation efficiency.

The main limitation of the char-forming materials is the rapid removal of the char in high-pressure, high-shear environments. Under these conditions, it is difficult to maintain thick, stable chars because of the spallation caused by the thermal stresses, surface shear forces, and the internal stresses due to the gas pressure build-up within the char. These materials are being improved steadily by use of improved reinforcements (nylon, Refrasil, graphite) to give the char better strength properties.

The comparative ablation performance of phenolic and epoxy resins reinforced with materials such as graphite, carbon, silica, zinc chloride, titanium dioxide, nylon, asbestos, etc., has been determined for a variety of environmental conditions.[4–7] An important conclusion from these studies is that the comparative ablation performance depends

Received December 16, 1963; revision received May 26, 1964. This work was sponsored by the Ballistic Systems Division of the U. S. Air Force under Contract No. AF 04(694)-222. The author wishes to acknowledge Paul Gordon and Charles Grebey for their assistance in the numerical analysis and programing of the equations for the IBM 7094 digital computer. The author also wishes to express his appreciation to other colleagues in the Space Sciences Laboratory and members of the Re-Entry Systems Department for their helpful discussions.

* Specialist, Gas Dynamics, Missile and Space Division, Space Sciences Laboratory. Member AIAA.

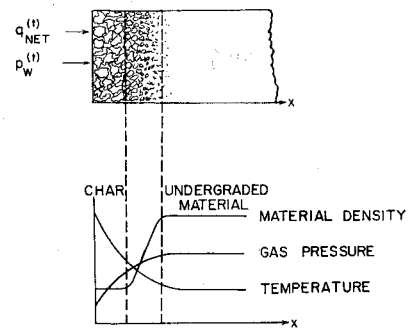

Fig. 1 Schematic diagram of charring ablator.

strongly upon the environmental conditions to which it is exposed. At present, there is no one material that performs well under all conditions.

Mechanical spallation appears to be one of the important mechanisms for the char removal of modified epoxies, phenolic nylon, phenolic graphite, and similar char-forming materials.[7–11] The spallation appears to be caused by the stresses associated with the pressure drop through the char material due to the internal pressure build-up of the degradation gases. The surface shear stresses also play an important role in the high shear environments.

One of the first studies of the mechanical removal of the char surface was performed by Dhanak.[12] The results are limited since the thermodynamic aspect of the problem is neglected. Parameters, which were obtained from a dimensional analysis, were combined with a simplified boundary-layer analysis in an attempt to determine the effect of the surface recession and ultimate shear strength on the boundary-layer characteristics. It was postulated that the char material shears off continuously when the local surface shear stress exceeds the ultimate shear strength of the material.

More recently, Scala and Gilbert[13] determined the ablation characteristics of a typical char-forming material that undergoes char removal by mechanical spallation. The chemical and thermodynamic aspects of the ablation process were considered along with the mechanical and thermal stresses. The results are based upon a quasi-steady state analysis. Such conditions are not realistic since the spallation phenomena as well as the environmental conditions for a typical re-entry trajectory are truly transient in nature.

In order to improve the understanding and to provide additional insight into the spallation phenomena, a study of the transient thermal response and ablation performance of charring ablators was conducted. The physical ablation model considered and the governing differential equations have been described in Ref. 14. The heat-protection material is treated as a "continuous" layer,[15] i.e., the final char material, reaction zone, and original plastic material are treated as one continuous layer (Fig. 1). The thermodynamic and mechanical properties of the material and gases change in a continuous manner through the material. Such a formulation permits a detailed description of the thermal response of the material and of the gas pressure build-up within the material.

The purpose of this paper is to present analytical results for the transient thermal response of a castable ablation resin[8, 16] for which spallation plays an important role in the char removal. The effects of porosity, critical stress, heating rate, and order of degradation reaction are shown.

Governing Equations

The governing equations for the thermal response of a char-forming material are taken to be the Arrhenius kinetics equation for the degradation of the original material, the thermal energy equation for the gas-char combination, and the continuity, momentum, and state equations for the degradation gases.

In the present calculations, the local rate of change of gas density with respect to time is neglected. This allows the temperature and mass flux of gases to be determined, and from these quantities the gas pressure distribution through the material is then determined. This is an approximation to the full coupled pressure-temperature analysis as formulated in Ref. 14.

Energy Equation

The thermal energy per unit bulk volume of the gas-char combination is governed by a one-dimensional heat balance equation

$$(\rho C_p)_{\text{eff}} \frac{\partial T}{\partial t} + \dot{m}_g C_{p_g} \frac{\partial T}{\partial x} = \frac{\partial}{\partial x}\left(k_{\text{eff}} \frac{\partial T}{\partial x}\right) + \dot{W}_p H_R \quad (1)$$

where

$$k_{\text{eff}} = f k_g + (1 - f) k_s$$

$$(\rho C_p)_{\text{eff}} = f \rho_g C_{p_g} + (1 - f) \rho_s C_{p_s}$$

The respective terms in the energy equation represent the heat stored, heat convected, heat conducted, and heat absorbed during the degradation process. The work done on the gas by the pressure forces and the viscous dissipation effects are neglected.

Degradation Kinetics

The thermal degradation of the original plastic material is given by[17]

$$\dot{W}_p(x, t) = \frac{\partial \rho_p}{\partial t} = -A e^{-E/RT} \rho_{VP} \left(\frac{\rho_p - \rho_c}{\rho_{VP}}\right)^n \quad (2)$$

where ρ_p is the instantaneous bulk density of material.

The frequency factor, activation energy, and order of reaction are determined from experimental results.

Mass Flux of Degradation Gases

The mass flux of gases is given by

$$\dot{m}_g(x, t) = \int_x^L \Gamma \dot{W}_p(x, t) dx \quad (3)$$

This neglects the local rate of change in gas density with respect to time. Thus, degradation gases, which are formed within the material, instantaneously flow through the surface.

Gas Pressure

The pressure distribution through the material is given by

$$p^2(x, t) = p_w^2(t) - 2 \int_0^x \frac{RT}{\bar{M}K} \dot{m}_g \, dx \quad (4)$$

This equation is obtained from the equation of state and the momentum equation, which assumes that the gas velocity is proportional to the pressure gradient. The proportionality factor is the permeability. The permeability, as well as the porosity, are taken to be functions of the instantaneous material density

$$K = K_c \left(\frac{\rho_p - \rho_{VP}}{\rho_c - \rho_{VP}}\right) \qquad f = f_c \left(\frac{\rho_p - \rho_{VP}}{\rho_c - \rho_{VP}}\right) \quad (5)$$

The permeability and porosity of the mature char are also determined from experiments.

Solution of Equations

Equations (1–4) were solved by a numerical finite-difference scheme on the IBM 7090 digital computer. The tem-

perature, mass flux of gases, and material density are determined from Eqs. (1–3). The gas pressure is then determined from Eq. (4) by simple quadrature.

The boundary conditions for the temperature equation are given by the net heat flux at the surface

$$q_{net}(o, t) = -k_{eff}(\partial T/\partial x) \quad (6)$$

In these calculations, the convective, hot-gas radiation, surface reradiation, and mass addition heat fluxes are considered in determining the net heat flux to the surface.

The appropriate heat flux is used at the back face; i.e., the heat flux is made continuous with the heat flux associated with an insulation layer, or a zero heat flux for the case of no heat transfer.

Spallation Criteria

The mechanisms by which char is removed or the surface recedes are not well understood. In these calculations, the char is assumed to be removed by a spallation process. Two possible mechanical effects are considered. One is the aerodynamic shear stress and the other is the normal stress associated with the gas pressure build-up within the material. Actually, the shear and normal stresses act together to cause the mechanical failure and removal of the char.

In the higher shear environments, there are indications that the char layer is sheared when its thickness reaches a critical value.[7] An empirical relation that relates the critical char thickness to the shear stress acting on a nonablating surface has been given by Tavakoli[18]:

$$\delta_c = B_1/(B_2 + \tau) \quad (7)$$

where B_1 and B_2 are constants that are determined from tests for each material. Actually, this relation includes the effects of thermal and gas pressure stresses as well, since these effects were present in the tests from which the empirical result was obtained.

Equation (7) is used as one of the spallation criteria in the present calculations. The surface shear stress is known from the environmental condition as a function of time. Therefore, the critical char thickness is known as a function of time. If the calculated char thickness exceeds the critical value, the char layer is spalled.

The char layer is also spalled by the gas pressure build-up that occurs within the material. One explanation attributes the spallation to the increased flow resistance close to the hot surface.[7, 8] The gases that are generated by the degradation of inner layers must flow to the surface through the hot porous char. The outer char is at a higher temperature. Accordingly, some of the degradation gases are "cracked," and carbon is deposited on the char. This causes a pressure build-up, a time-dependent phenomenon, inside the ablating surface, and the char eventually spalls because of the relatively high internal stresses.

In the present analysis, the pressure build-up is due to the normal resistance of the char to the flow. Actually, the densification effects are not included since the porosity increases as the surface is approached. Also, only one degradation reaction, which occurs over a relatively narrow range of temperatures, is considered.

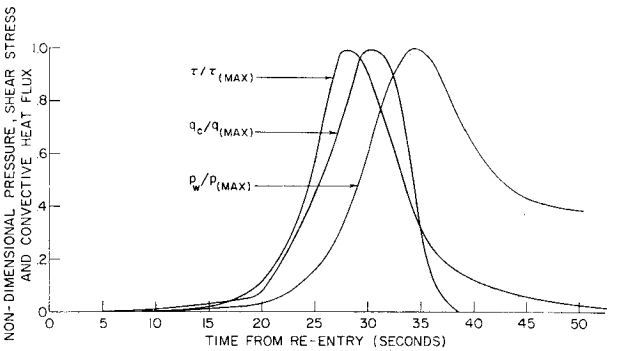

Fig. 2 Environmental conditions.

The normal stress due to the pressure drop through the material is given by

$$\sigma = pf - p_W \quad (8)$$

This stress is based upon the total cross-sectional area.

Equation (8) is also used as a spallation criteria in these calculations. If the calculated stress exceeds an assumed failure stress of the char, the char is spalled.

Both the critical char thickness and normal failure stress criteria are used. The material is spalled when the critical value of either is reached.

Application to Re-Entry Environment

For illustrative purposes, calculations were performed for a representative sphere-cone ballistic re-entry vehicle. Typical results for the transient thermal response of the heat protection material during the re-entry heating cycle are presented for one axial location on the vehicle.

Environmental Conditions

The environmental conditions (convective heat flux, pressure, shear stress) to which the surface of the vehicle is exposed are presented in Fig. 2. The values for the axial location chosen are

$$q_{max} = 367 \frac{\text{Btu}}{\text{ft}^2\text{-sec}} \qquad p_{max} = 2500 \text{ psf} \qquad \tau_{max} = 29 \text{ psf}$$

Material and Gas Properties

The heat protection material considered is a high-performance castable epoxy resin,[8] which is representative of a charring ablator for which spallation is an important mechanism in the char removal. The important material and gas properties are given in Table 1.

Actually, quantities such as specific heat, thermal conductivity, and molecular weight are tabulated as functions of temperature and used in the calculations. For example, the molecular weight of the degradation gases is taken to be 72 lb/mole at the low temperature and 20 lb/mole at the higher temperatures. This variation in molecular weight is extremely important in determining the heat-blocking effect since the lower molecular weight gases are more effective.

Table 1 Properties of materials and gaseous products

Virgin plastic	Char	Gases
$\rho_{VP} = 75$ lb/ft^3	$\rho_c = 22$ lb/ft^3	
$k_{VP} = 3.82 \times 10^{-5}$ Btu ft-sec-°R	$k_c = 2.4 \times 10^{-4}$ Btu/ft-sec °R	$k_g = 5 \times 10^{-6}$ Btu/ft-sec-°R
$C_{pVP} = 0.423$ Btu/lb-°R	$C_{pc} = 0.5$ Btu/lb-°R	$C_{pg} = 0.4$ Btu/lb-°R
$H_R = 100$ Btu/lb	$K_c = 1.8 \times 10^{-5}$ ft^4/lb-sec	$\bar{M} = 20$–72 lb/mole
$A = 1.1 \times 10^5$ sec^{-1}	...	...
$\Delta E = 36.9 \times 10^3$ cal/mole	...	...
$n = 2$	...	...

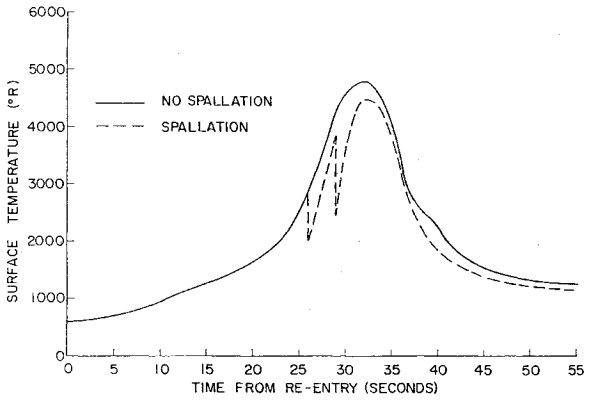

Fig. 3 Surface temperature history.

Numerical Results

Results for the over-all ablation performance are given in Figs. 3–8. In order to show the importance of retaining the char layer, the spallation results are compared with the results for the case of no spallation, i.e., no char removal.

The surface temperature history (Fig. 3) indicates clearly the rapid change in surface temperature during spallation. The maximum surface temperature with spallation is 4420°R as compared with 4800°R without spallation. The effectiveness of the char layer as a thermal barrier is reflected in the higher surface temperature and also in the smaller degradation depth when the char layer is retained (Fig. 4). This also results in a lower backface temperature, which is important in designing the substructure.

Two spallations, which are evidenced by the two discontinuous decreases in temperature, occurred. The spallation is also noticeable in the surface recession (Fig. 4), which occurs in a stepwise manner.

Detailed calculations of the temperature, gas pressure, material density, porosity, and normal stress distributions through the material are presented for the time at which the first spallation occurs (Fig. 5) and the second spallation (Fig. 6). In both cases, the surface is being heated quite rapidly.

The mature char layer is much thinner than the degradation zone layer. In these calculations, the thickness of material removed at each spallation is equal to the degradation thickness. This results in the removal of approximately twice the mature char thickness each time. Thus, it is expected that the calculation will overpredict the surface recession. On the other hand, the maximum internal stress due to the gas pressure occurs below the mature char, and it is likely that the surface layer will fail near this location, especially since the material is also in a very plastic state in this region of the degradation zone.

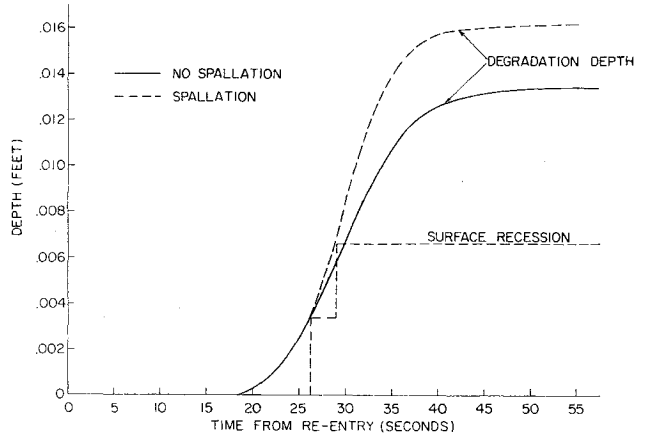

Fig. 4 Degradation and ablation depths.

A critical normal stress of 500 psf was assumed in these calculations. The maximum internal stress due to the gas pressure build-up was 313 psf at the beginning of the first spallation and 261 psf at the second spallation. Therefore, the critical normal stress was not the governing spallation factor. Rather, the spallation was controlled by the critical char thickness as related to the surface shear stress. The value of the shear stress was 25 psf for the first spallation and 28 psf for the second spallation. A second set of calculations was performed for an assumed critical stress of 300 psf. As expected, the first spallation was governed by the critical stress and the second by the critical char thickness. The final degradation depths and surface recessions agreed within 4%. The spallation period was on the order of 2.25 sec in both cases.

The mass flux of degradation gases entering the external flow (Fig. 7) is very irregular due to the spallation of the char. When the char is removed, the virgin material is exposed to a

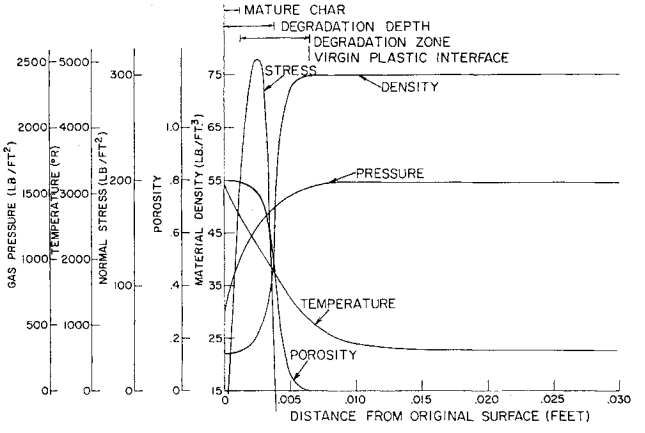

Fig. 5 Variation of properties through material, first spallation.

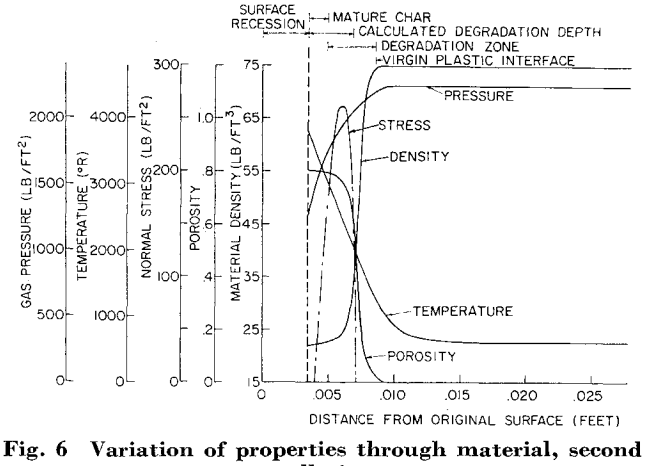

Fig. 6 Variation of properties through material, second spallation.

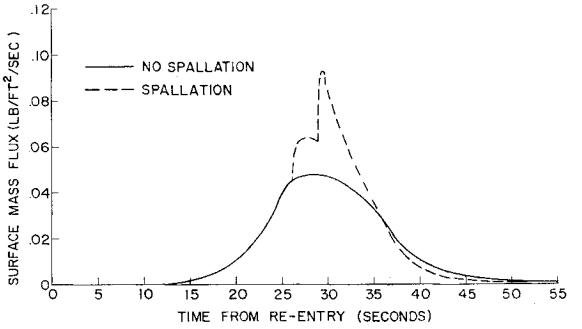

Fig. 7 Mass flux of degradation gases.

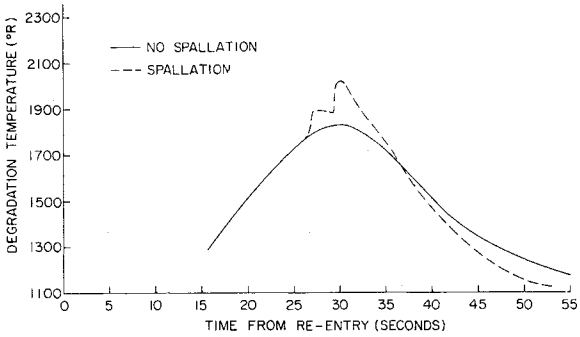

Fig. 8 Degradation temperature.

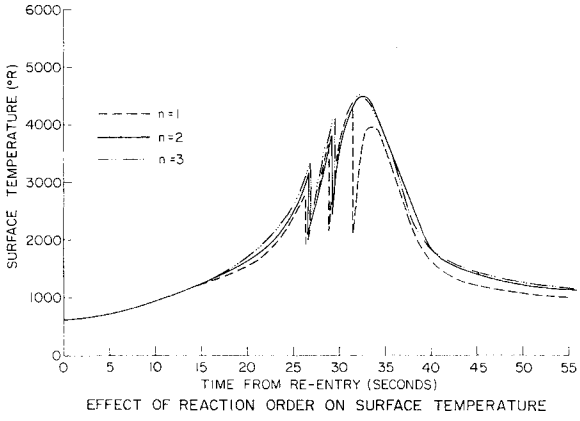

Fig. 9 Effect of reaction order on surface temperature.

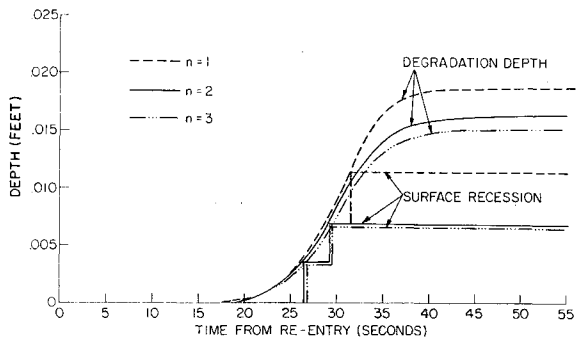

Fig. 10 Effect on reaction order on degradation and ablation depths.

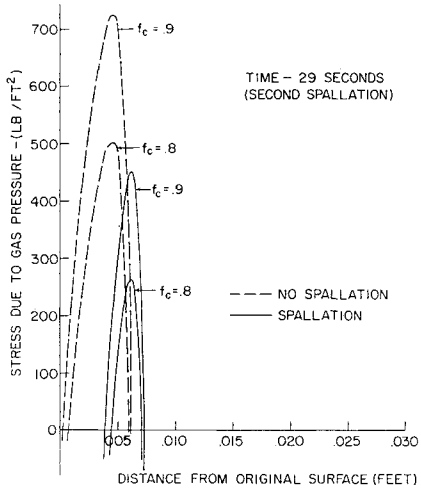

Fig. 11 Effect of porosity on internal stress.

new increased heat flux, and the amount of degradation gases given off increases rapidly. The maximum value of the mass flux increased by a factor of 2. This is important in determining the heat blocking and the effects of the degradation gases on the high-temperature boundary-layer flow.

The char-forming materials do not degrade thermally at a definite temperature. Rather, the degradation occurs over a temperature range. In fact, it is very likely that the degradation process should be represented by several processes, each occurring over a different temperature range.[8, 17] Also, the temperature at which the maximum degradation occurs is not a constant (Fig. 8). It is affected by the heating rate and varies considerably throughout the trajectory. These calculations show that the degradation temperature varies from 1200° to 2000°R during the heating cycle. One of the limitations of an "interface" ablation analysis is the fact that a constant degradation temperature is assumed. A value of 1710°R was used in an analysis by Swann[19] and a value of 1310°R in calculations performed by Schmidt.[9]

The heat of ablation, based upon the integrated convective heat flux and total material ablated, is 5000 Btu/lb for no spallation as compared to 3500 Btu/lb for the spallation case. This again shows the effectiveness of maintaining a thick char.

Order of Degradation Reaction

The order of the degradation reaction is rather difficult to determine from experiments. Therefore, calculations were also performed for first-order and third-order reactions to determine the sensitivity of the results. The surface temperature (Fig. 9) is relatively insensitive. For the first-order reaction, a third spallation occurred (Fig. 10) because the material degraded more rapidly for the lower-order reaction, and consequently the critical char thickness was reached sooner. Also, larger stresses occur for the lower-order reactions.

The effect on the internal stress and the instantaneous char thickness is summarized in Table 2. All of the spallations were governed by the critical char thickness since the stresses did not reach the assumed value of 500 psf for the failure stress.

Effect of Char Porosity on Stress

The stress due to the gas pressure drop through the char is an important factor in the spallation process. It is very much dependent upon the char porosity. Therefore, calculations were also carried out for a value of the mature char porosity equal to 0.9. Results for the stress are presented in Fig. 11 at the beginning of the second spallation, which occurred 29 sec after the start of the heating cycle.

A change in the porosity has a large effect on the internal stress. As the porosity increases, the internal surface area that the gas pressure acts on also increases.

Table 2 Effect of reaction order on stress and char thickness

	$n = 1$		$n = 2$		$n = 3$	
	Stress, psf	Char thickness, ft	Stress, psf	Char thickness, ft	Stress, psf	Char thickness, ft
First spallation	456	0.0039	313	0.0038	245	0.0037
Second spallation	396	0.0033	261	0.0034	142	0.0034
Third spallation	185	0.0044	...	...	...	...

Table 3 Summary of increased heat flux results

	Normal heat flux	Increased heat flux	
	σ_F = 500 psf	σ_F = 500 psf	σ_F = 1000 psf
Spallation mechanism	Critical char thickness	Critical stress	Critical char thickness
No. of spallations	2	13	4
Spallation period	2.25 sec	2.14–0.48 sec	2.27–1.65 sec
Degradation depth	0.0163 ft	0.0291 ft	0.0244 ft
Surface recession	0.00687 ft	0.0257 ft	0.0151 ft
Peak surface temperature	4420°R	5300°R	5358° R
Maximum mass flux of gases	0.092 lb/ft²-sec	0.309 lb/ft²-sec	0.15 lb/ft²-sec

In the case of no spallation, the stresses are distributed over a greater depth since the char and degradation layers are thicker. Also, the stresses are much higher, since the degradation gases have much more resistance to overcome in flowing through a larger thickness of porous material.

The stresses at the beginning of the heating cycle and during the end are entirely compressive. During the beginning of the cycle, relatively small amounts of gases are flowing, and the material is not very porous. Therefore, the compressive stress is due to the aerodynamic pressure acting on the surface. During the latter portion of the heating cycle, the material is quite porous but the surface pressure is large, such that the pressure drop is rather small even though a considerable amount of gases is flowing through the porous material. The resulting compressive stresses are relatively large. For these cases, the stresses are on the order of 1500 psf. Thus, it appears possible for some of the char to be removed and blown away by a crushing reaction.[3]

Increased Heat Flux

The convective heat flux was increased by a factor of 1.65 such that q_{max} = 605 Btu/ft²-sec. The other environmental quantities were not changed. Calculations were performed for a failure stress of 500 psf. The results are summarized in Table 3.

A failure stress of 500 psf resulted in the removal of char in 13 spallations, which are quite evident in the stepwise progression of the surface recession (Fig. 12). All of the spallations were governed by the critical stress. The first spallation period is 2.14 sec. This decreases to 0.48 sec near peak heating and then increases to a value of 1 sec for the last spallation period.

For a failure stress of 1000 psf, four spallations occurred, and each was governed by the critical char thickness. The maximum internal stress at each spallation was approximately 700 psf.

It is evident that a knowledge of the failure stress of chars is essential in determining the surface recession, since the surface recession increased by 70% if the failure stress is changed from 700 to 500 psf. The degradation depth changed by 19%, but the maximum surface temperature was essentially the same.

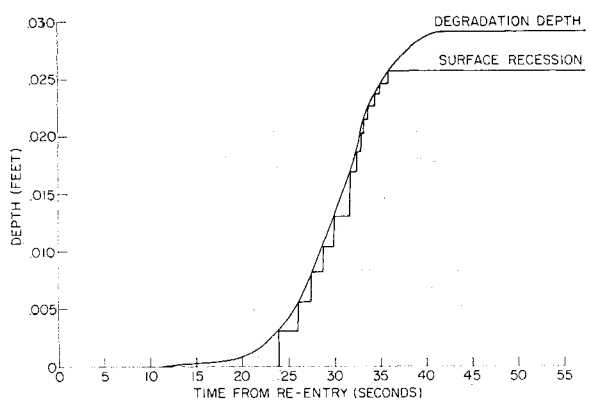

Fig. 12 Degradation and ablation depths (increased heat flux).

The thermal protection provided by the char layer decreases as the char is removed more rapidly, and the mass flux of degradation gases increases considerably. An accurate knowledge of the mass flux is necessary in determining the boundary-layer flow characteristics.

Concluding Remarks

The removal of char by a spallation process has been included in a transient ablation analysis of a typical charring ablator exposed to re-entry environmental conditions. The stepwise progression of the surface recession due to the periodic spallation and the corresponding surface temperature changes have been calculated. Detailed calculations of the degradation depth, surface mass flux of gases, degradation temperature, and variation of temperature, material density, internal stress, gas pressure, and porosity through the material have also been presented.

The maximum stress due to the gas pressure drop occurs below the mature char layer. In this degradation zone, the material is in a plastic state, and it is very likely that the material fails in this region. Recent stress calculations, which take into account the thermal and pressure effects in a porous cylindrical char layer, show that the radial location of the maximum radial stress is not affected significantly by the thermal effects.[20]

The results depend upon an accurate knowledge of the mechanical, chemical, and thermodynamic properties of the gases and material. Most of these quantities must be determined experimentally. Some are known to a much better degree of certainty than others. The need for improving the knowledge of the chemical degradation process is still present. The present calculations demonstrate the need for determining the char properties (porosity, permeability, failure stress) more accurately for materials that spall.

The present stress calculation should be extended to include the thermal and surface shear stresses. Then the spallation can be based upon one failure stress and the critical char thickness criterion eliminated.

Other char-removal mechanisms, such as oxidation and sublimation at the higher temperatures, should be included since these can be significant under the appropriate conditions. Also, an attempt should be made to include the densification of the outer char due to the cracking of the degradation gases. This will result in increased gas pressures due to the increased flow resistance of the char.

The analysis upon which these calculations is a first approximation to the coupled pressure-temperature analysis.[14] The coupled problem can also be performed with the present analysis by including the unsteady term in the continuity equation as a higher approximation. Results from the first approximation can then be used to solve the resulting equations by an iteration procedure.

References

[1] Steg, L. and Lew, H. G., "Hypersonic ablation," AGARD Hypersonic Conference, TCEA Rhode-St. Genese, Belgium (April 3–6, 1962); also General Electric Co., Missile and Space Div., TIS-R62SD55 (May 1962).

[2] Hurwicz, H., "Aerothermochemistry studies in ablation," Fifth AGARD Combustion and Propulsion Colloquium, Brunswick, Germany (April 9–13, 1962).

[3] Schmidt, D. E., "Ablation of plastics," Aeronautical Systems Div. TR-61-650 (February 1962).

[4] Buhler, R. D., Christensen, D., and Grindle, S., "Effects of hyperthermal conditions on plastic ablation materials," Aeronautical Systems Div. TR-61-304, Plasmadyne Corp., (January 1962).

[5] Mixer, R. Y. and Marynowski, C. W., "A study of the mechanism of ablation of reinforced plastics," Wright Air Development Center TR 59-668, Part I (February 1960).

[6] Barry, W. T. and Sutton, W. H., "The importance of char structures in the ablation performance of organic polymers," General Electric Co., Missile and Space Div., TIS-R60SD329 (March 11, 1960).

[7] Robbins, D. L., "Thermal erosion of ablative materials," Aeronautical Systems Div. TR-61-307, Aerojet-General Corp. (April 1962).

[8] Barry, W. T. and Gaulin, C. A., "A study of physical and chemical processess accompanying ablation of G.E. century resins," General Electric Co., Missile and Space Div., TIS-R62SD2 (May 1962).

[9] Schmidt, D. L., "Behavior of plastic materials in hyperthermal environments," Wright Air Development Center TR 59-574 (April 1960).

[10] Myers, H. and Harmon, D., Jr., "Energy transfer processes in decomposing polymeric systems," Engineering Paper 1020, Missile and Space Systems Engineering, Douglas Aircraft Co. (September 1960).

[11] Vojvodich, N. S. and Pope, R. B., "Effect of gas composition on the ablation behavior of a charring material," AIAA J. **2**, 536–542 (1964).

[12] Dhanak, A. M., "A theoretical study of mechanical erosion from a charred surface in boundary layer flows," AVCO RAD-7-TM-60-74 (December 1960).

[13] Scala, S. M. and Gilbert, L. M., "Thermal degradation of a char-forming plastic during hypersonic flight," ARS J. **32**, 917–924 (1962).

[14] Mathieu, R. D., "Response of charring ablators to hyperthermal environment," General Electric Co., Missile and Space Div., TIS-R63SD20 (February 1963).

[15] Munson, T. A. and Spindler, R. J., "Transient thermal behavior of decomposing materials, Part I, General theory and application to convective heating," IAS Paper 62-30 (January 1962).

[16] Friedman, H. L., "The pyrolysis of plastics in a high vacuum arc image furance," General Electric Co., Missile and Space Div., TIS-R62SD57 (December 1962).

[17] Friedman, H. L., "The kinetics of thermal degradation of charring plastics," General Electric Co., Missile and Space Div., TIS-R61SD145 (August 1961).

[18] Tavakoli, M. L., private communication (November 1961).

[19] Swann, R. T. and Pittman, C. M., "Numerical analysis of the transient thermal response of advanced thermal protection systems for atmospheric entry," NASA TN D-1370 (July 1962).

[20] Menkes, E. G., "Analysis of the structural behavior of charring ablator heat protection systems," General Electric Co., Missile and Space Div. (to be published).

SEPTEMBER 1964 AIAA JOURNAL VOL. 2, NO. 9

Time for a Totally Wetting Liquid to Deform from a Gravity-Dominated to a Nulled-Gravity Equilibrium State

HOWARD L. PAYNTER*
Martin Company, Denver, Colo.

This article presents an analytical method to predict the time required for a liquid/vapor system to deform from a gravity-dominated condition to that of a nulled-gravity equilibrium state. The theoretical analysis assumes that the free surface is completely transformed to kinetic energy during this deformation. The physical model is a spherical container partially filled with a totally wetting liquid. A dimensionless coefficient, a function of tank radius only, was then employed to modify the theoretical analysis and to provide good correlation between analytical results and NASA experimental data.

Nomenclature

SE = surface energy, ft-lbf
KE = kinetic energy, ft-lbf
H = correlation coefficient
σ = surface tension, lbf/ft
R, r = radius, ft or cm
R_c = constant, 1 cm
v = velocity, fps
m = mass, lbm
ρ = mass density, lbm/ft^3
τ_p = zero-g elapsed time parameter, dimensionless
τ = time, sec
g_c = 32.174 lbm-ft/lbf-sec^2
V = volume, ft^3
K = Harkins' spreading coefficient
ξ = ratio, liquid-to-container volume
β = kinematic surface tension, ft^3/sec^2

Subscripts

l = liquid
n = refers to the nth increment ($1 \leq n \leq 30$)
lv = liquid/vapor
sv = solid/vapor
sl = solid/liquid
0 = initial

Received October 21, 1963; revision received May 18, 1964.

* Design Specialist, Advanced Development and Technology Section, Propulsion and Mechanical Engineering Department. Member AIAA.

Introduction

ZERO-GRAVITY, and associated fluid problems, are discussed in Refs. 1–4. A particular problem for the designer of liquid rocket engines is predicting the time required